

promoting access to White Rose research papers



Universities of Leeds, Sheffield and York
<http://eprints.whiterose.ac.uk/>

This is an author produced version of a paper published in **Surface and Coatings Technology**.

White Rose Research Online URL for this paper:
<http://eprints.whiterose.ac.uk/4934/>

Published paper

Rybiak, R., Fouvry, S., Liskiewicz, T. and Wendler, B. (2008) *Fretting wear of TiN PVD coating under variable relative humidity conditions – development of a “composite” wear law*. *Surface and Coatings Technology*, 202 (9). pp. 1753-1763. ISSN 0257-8972

<http://dx.doi.org/10.1016/j.surfcoat.2007.07.103>

Fretting wear of a TiN PVD coating under variable relative humidity conditions – development of ‘composite’ wear laws

R. Rybiak^{a,b}, S. Fouvry^{a,*}, T. Liskiewicz^{a,b}, B. Wendler^b

^a *Laboratoire de Tribologie et Dynamique des Systèmes, CNRS UMR 5513, Ecole Centrale de Lyon, 36 Avenue Guy de Collongue, 69134 Ecully Cedex, France*

^b *Institute of Materials Engineering, Technical University of Lodz, Stefanowskiego 1, 90924 Lodz, Poland*

* *Corresponding author (Siegfried.Fouvry@ec-lyon.fr)*

Abstract

Fretting is defined as a small oscillatory displacement between two contacting bodies. The interface is damaged by debris generation and its ejection from the contact area. The application of hard coatings is an established solution to protect against fretting wear. For this study the TiN hard coating manufactured by a PVD method has been selected, and tested against a polycrystalline alumina smooth ball. A fretting test programme has been carried out at a frequency of 5 Hz, 100 N normal load, 100 μm displacement amplitude and at five values of relative humidity: 10, 30, 50, 70 and 90% at a temperature of 296 K. The intensity of the wear process is shown to be significantly dependent on the environmental conditions. A dissipated energy approach has been employed in this study to quantify wear rates of the hard coating. The approach predicts wear kinetics under constant medium relative humidity in a stable manner. It has been shown that an increase of relative humidity promotes the formation of hydrate structures at the interface and modifies the third body rheology. This phenomenon has been characterised by the evolution of wear kinetics associated with a significant variation of the corresponding energy wear coefficient. Hence, a ‘composite’ wear law, integrating the energy wear coefficient as a function of relative humidity, is introduced. It permits a prediction of wear under variable relative humidity conditions from 10 to 90% within a single fretting test. The stability of this approach is demonstrated by comparing various variable relative humidity sequences.

1. Introduction

The use of hard ceramic coatings can significantly improve the tribological properties of cutting tools and mechanical components [1-18]. It permits an extension of their lifetime and contributes to higher working efficiency. Even though TiN coatings have been commonly and widely used for commercial applications, there is still a great interest in obtaining an in-depth characteristic of their wear damage under various conditions.

Many researchers have investigated the impact of different relative humidity (RH) on friction and wear behaviour of the TiN coatings. Singer et al. [1] were the first who employed the full power of modern electron microprobes to characterize the formation and chemistry of wear debris on a ball on disc test in ambient air, under medium relative humidity. The low friction coefficient observed at the beginning of the test, with a sapphire ball against TiN, was attributed to easy shear at the TiO_{2-x} -TiN interface. The study conducted by Mohrbacher et al. [2] on the fretting behaviour of TiN coatings demonstrated that there is a significant modification of the friction behaviour at different RH levels. Low friction, observed at a high relative humidity, independently of the counter-body material (corundum or steel), was inferred again to the formation of TiO_{2-x} lubricious layers through the interface. It has been established that a high content of moisture in the atmosphere accelerates the reaction between TiN and oxygen during the fretting loadings and favours the formation of TiO_{2-x} components, which decreases the friction coefficient. Using micro-Raman spectra it has been shown that the coefficient of friction of TiN coatings depends on the structure of the debris, which can either take the form of anatase or rutile structure [2-3]. Additionally, transmission electron microscope investigations indicated that a low coefficient of friction obtained at high RH could be related to the two-phase debris consisting of an amorphous and a nanocrystalline rutile phase. On the other hand, high coefficients of friction, characteristic for low RH conditions, have been related to the absence of nanocrystalline rutile phase [3]. Another study conducted by de Wit et al. [4] on fretting wear of the TiN-corundum system at medium RH

revealed an amorphous Ti-O-(N) two-phase debris structure. The characteristic drop of the friction coefficient observed during fretting tests has been attributed to the partial transformation of amorphous debris into a nanocrystalline phase. This transformation is a result of combined effect of relative humidity, energy-input and the continuous oxidation of titanium-oxy-nitride.

The mentioned works consider only the friction and wear behaviours of TiN coatings under constant relative humidity conditions. However, in practice most mechanical systems operate under variable mechanical but also variable environmental conditions. It has been shown by Liskiewicz et al. [5] that the relative humidity in different geographical locations in Europe can vary more than 50% within a two weeks period. Hence, it appears that an adequate evaluation of the tribological behaviour of the mechanical systems requires taking into account variable environmental conditions.

The present work will focus on this peculiar aspect, and will show how a basic energy wear approach can be transposed to capture the wear kinetics under variable relative humidity conditions.

2. Experimental Section

2.1 Materials

The TiN coating manufactured by means of classical single source Arc-PVD method has been tested against polycrystalline alumina ball (radius $R=12,7$ mm). The substrate material is a sintered Vanadis 23 steel with the following chemical composition: 1,28 wt.% C; 4,2 wt.% Cr; 5,0 wt.% Mo; 6,4 wt.% W and 3,1 wt.% V. Figure 1 displays the X-Ray diffraction pattern of the TiN coating with (111) planes parallel to the coating surface. The angular position of the diffraction peak meets the standard value of the corresponding stoichiometric TiN phase.

An alumina ball has been selected as a counter-body, because it limits chemical and adhesive interactions with TiN layer [5-7]. Indeed, a conventional steel counter-body is chemically

active and can cause unstable friction behaviour [1, 8-9]. Moreover, an application of alumina ball allows us to limit a counter-body impact on the complex tribo-system responses under variable RH situations.

The mechanical and surface properties of the studied materials are listed in Table I.

2. 2 Experimental procedure

Tests were carried out using a specific LTDS fretting wear apparatus (Fig. 2) in which an electrodynamic shaker induces the reciprocating movement. A constant 5 Hz frequency has been imposed. The upper specimen (alumina ball) rubbed against the lower fixed flat sample (steel coated with TiN). The normal force was kept constant, while the tangential force and displacement were recorded. A fretting test programme has been carried out applying a constant 100 N normal force of and constant $\pm 100 \mu\text{m}$ displacement amplitude. This loading promotes systematically gross slip sliding conditions. Considering an homogeneous steel/steel elastic hypothesis, the given contact leads to a maximum Hertzian pressure about 1.13 GPa and a contact radius about $206 \mu\text{m}$.

Tests were conducted in a closed chamber in which the relative humidity could be controlled. The measurement of humidity level has been performed as close as possible to the contact. Five different RH in the range from 10% (dry air), throughout intermediate 30, 50 and 70% up to 90% (wet air) have been considered in this work. In order to achieve required RH, granulated silica gel or water filled vessels have been adjusted within the chamber. A laboratory fan inducing an intense air circulation inside the chamber has been applied to accelerate the relative humidity transition.

Review of literature shows that probably no attention has been attached to the study under variable humidity conditions. Hence, a new methodology, taking into account the relative humidity variations within a test, has been designed. Dozen experiments under variable RH condition during a single fretting test have been carried out. They can be classified into 4 test configuration illustrated in Figure 3:

- type A characterised by RH increasing stepwise;
- type B described by RH decreasing stepwise;
- type C consisting of 2 repeated blocks: higher RH → lower RH;
- type D consisting of 2 repeated blocks: lower RH → higher RH.

Between each humidity transition the fretting tests were suspended for a short time interval (less than 10 minutes) in order to adjust the new RH value. Details of all tests conducted under variable relative humidity conditions are provided in Table II.

Before and after each test, specimens were ultrasonically cleaned with acetone. The wear volume of the fretting scars has been estimated from 2D surface profiles along and perpendicular to the sliding direction. A simplified integration has been employed to determine the wear volume of the fretting scars [10].

Scanning electron microscope (SEM) and energy dispersive X-ray spectrometry (EDX) analyses have been performed to get information regarding the chemical composition of wear debris. More advanced transmission electron microscope (TEM) investigations combining selected area electron diffraction (SAED) and electron spectroscopic imaging (ESI) have been carried out to characterize products of wear.

3. Results

3.1 Tribology behaviour under constant relative humidity conditions

3.1.1 Friction behaviour

Figure 4 depicts the evolution of the coefficient of friction (COF (μ)) as a function of the test duration for tests conducted at 10 and 90 % RH at 10k cycles. It can be observed an initial running-in period (first 2500 cycles) followed by steady-state behaviour. This steady-state evolution is related to stabilized wear debris formation and its ejection regime.

The evolution of the average values of the steady-state coefficient of friction ($\bar{\mu}_{ss}$) versus relative humidity defined by the relation:

$$\bar{\mu}_{ss} = \frac{1}{N - N_{ss}} \cdot \sum_{i=N_{ss}}^1 \mu(i) \quad (\text{eq. 1}),$$

with $N_{ss}=2500$ and $N=10000$ is plotted in Figure 5. The error bars represent the difference between maximum and minimum value recorded during this period. A linear decrease, from 0.65 at 10% RH to 0.50 at 90% RH can be observed. Hence, considering a linear approximation, a decrease of $\bar{\mu}_{ss}$ of the studied TiN/alumina interface versus the applied relative humidity can be formalized through the following relationship:

$$\bar{\mu}_{ss} = C_{\bar{\mu}_{ss}} \cdot (RH) + \bar{\mu}_{ss-0} \quad (\text{eq. 2}),$$

with $\bar{\mu}_{ss-0}$ – the mean steady-state coefficient of friction when RH=0% (presently extrapolated at 0.6209), $C_{\bar{\mu}_{ss}}$ – a slope of a linear approximation (identified at -0.1765), RH – relative humidity in %.

Values of the average steady-state coefficient of friction dependently on the applied relative humidity are depicted in Table III.

3. 1. 2 Wear behaviour

An energy approach has been employed to evaluate the fretting wear resistance of the studied TiN coating against alumina ball. Compared to the Archard [19] description which reflects the ratio of the total wear volume to the product of the normal force by the sliding distance, the energy wear approach includes the coefficient of friction through its formulation [10, 20-21]. Thus, it permits a more physical description of the fretting wear damage. Hence, the total wear volume (V) is related to the accumulated dissipated energy ($\sum E_d$) or the equivalent friction work. The accumulated dissipated energy is obtained by summing up the energy dissipated during each fretting cycle over the whole test duration. Numerous studies [5-6, 10,

14, 16] have shown that linear approximations can be extrapolated and from the slope of such evolutions, so-called energy wear coefficient (α) can be identified:

$$\alpha = \frac{\Delta V}{\Delta \sum E_d} (\mu\text{m}^3\text{J}^{-1}) \quad (\text{eq. 3}).$$

The energy wear coefficient appears as a unified factor which allows the characterization of the wear resistance of the tribo-couple independently of the applied loading conditions.

However, as it could be observed in Fig. 6, it seems to strongly depend on the relative humidity. Figure 7 displays a parabolic increase of the energy wear coefficient as a function of the relative humidity. The less is the value of the relative humidity of the air, the higher is the wear resistance. Above 70% RH threshold, a saturation effect can be observed, which can be associated to almost constant energy wear coefficients. On the contrary to the linear friction dependence, a parabolic evolution of the wear rate can be here deduced. The following formulation allowing its description can be introduced:

$$\alpha = C\alpha_1 \cdot (RH)^2 + C\alpha_2 \cdot (RH) + \alpha_0 \quad (\text{eq. 4}),$$

with $C\alpha_1 = -0.6564$, $C\alpha_2 = 109.88$, α_0 – value of energy wear coefficient when RH=0% (presently extrapolated at 661.52).

The corresponding energy wear coefficients (α) as well as the associated coefficients of determination (R^2) are compiled in Table IV.

The evolution of energy wear coefficient with the applied relative humidity supports the idea that modification of the nature and the structure of the third body with the relative humidity will significantly affect the energy balance of the damage phenomenon. Hence, in order to explain such wear rate dependence, it appears essential to probe the third body evolution as a function of the applied relative humidity.

3. 1. 3 Analysis of the wear debris structure

As previously mentioned in the introduction, numerous studies have outlined the relative humidity effect on the third body nature and consequently on the friction and wear responses. Basic SEM observations of the wear debris show that dry atmosphere promotes powder structures whereas moist atmosphere activates the formation of large glazed plates of the debris (Fig. 8). The latter one is more compliant and better maintained through the interface. These agglomerated structures act as lubricious layers adhering both on the ball and the plane surfaces. One explanation of this evolution could be related to the linking of oxides (TiO_2) with water molecules and the formation of adherent hydrate structures. To investigate such aspect, EDX analyses of the wear debris have been carried out. It has been shown that titanium (Ti), oxygen (O) and nitrogen (N) elements are present in all wear debris (Fig. 9). However, some differences have been found depending on the relative humidity. It can be observed that the amount of oxygen in the wear debris generated under moist conditions (90% RH) is higher than under dry air (10% RH). The oxygen/titanium concentration ratio is respectively 0.65 and 1.40 for dry and humid atmosphere. To confirm such results, EDX analyses of particles, using TEM, have been performed. They confirmed the presence of nitrogen in the wear debris as well as a significant increase of oxygen concentration in the debris obtained under moist conditions (Fig. 10). Such results again support the hypothesis that moist atmosphere may promote the formation of complex titanium oxide – hydrate structures ($\text{TiO}_2 - \text{H}_2\text{O}$). The presence of water molecules obviously increases the oxygen/titanium ratio as well as modifies the surface energy of particles favouring their agglomeration and the formation of macro – lubricious glazed layers. The presence of nitrogen element in the wear debris also suggests that rather Ti-O-(N) complex structure [4] than only TiO_2 phases are generated through the interface. In addition, SAED investigations of the wear debris have been performed. Figure 11 depicts the electron diffraction pattern obtained just after switching the electron gun on and after 5 minutes of electron irradiation. It

is worth to note that similar patterns have been obtained both under moist (90% RH) and dry (10% RH) conditions. Only weak halo related to an amorphous phase can be distinguished at the initial stage of the observation. However, after a few minutes of irradiation, the amorphous phase is progressively crystallized due to the input energy provided by the electron beam. The given analysis seems to refute the previous conclusions concerning the presence of incipient nanocrystalline structure in wet debris [3]. Indeed, only amorphous structures have been detected at the incipient stage of the TEM observations, whereas crystalline structures have been systematically observed after a few minutes of irradiations. It therefore outlines the necessity to take into account the probe perturbations associated to the material expertise. It suggests that careful experimental procedures must be implemented when unstable amorphous structures are characterized. More in-depth investigations involving XPS and Raman techniques are currently planned in order to clarify the present disagreement with hypothesis put forward by Wit et al. [3], but also to rationalize the proposed TiO₂ hydratation theory.

3. 2 Tribology behaviour under variable relative humidity conditions

Based on the previous analysis, the contact behaviour under complex and variable relative humidity conditions (A, B, C and D test types as defined in Figure 3) will be investigated.

3. 2. 1 Friction Behaviour

Figure 12 plots the COF evolutions obtained for the representative loading conditions A1, B1, C1 and D1. The experimental results are compared with the theoretical evolutions extrapolated from the constant humidity friction responses ($\bar{\mu}_{ss}$ for the given RH level). Some divergences between them can be observed. Besides, characteristic discontinuities after each change of RH, attributed to the short detention intervals, are of course visible. Specific

evolutions can be observed depending on the imposed ambient sequences. Hence, the smooth decrease of the friction coefficient within a sequence at 90% RH for the test D1 can be related to a ‘friction memory effect’. Indeed, a given time is required before the formation of a low friction layer takes place. The enriched in oxygen lubricious layer is progressively activated by the moist air. It may be assumed that after a longer time period a stable condition is reached equivalent to a constant humidity value. This aspect requires more in-depth experimental validations where longer step, within the level of 90% RH, must be carried out. Regarding the C1 test, an increase of the COF for each increment of 10% RH is observed. Such behaviour can be explained by a mutual interaction of a higher amount of the debris transferred on to the ball surface during the former step at 90% RH [5] and the debris depletion in oxygen after the transition to a dry environment. Hence, one hypothesis is that after decreasing the relative humidity the debris instead of acting as a lubricious layer, adheres on to the ball surface and operates like abrasive and promotes a friction forces increase. Evolutions of coefficients of friction for tests A1 and B1 can be accounted for based on the formulated above deduction concerning tests C1 and D1.

More in-depth investigations, which cannot be performed through the global overview of this work, are indeed required to interpret and quantify the interface evolutions induced by the humidity variations and to better formalize the dry to wet and reverse wet to dry transitions. Finally, by considering a regular evolution of the steady-state coefficient of friction, an average formulation involving the RH fluctuation ($\bar{\mu}_{ss-RH}$) can be introduced:

$$\bar{\mu}_{ss-RH} = \frac{1}{(N - N_{ss})} \cdot \sum_{i=N_{ss}}^N \mu_i(RH(i)) \quad (\text{eq. 5}),$$

with N – test duration in cycles, $N_{ss} = 2500$ cycles.

Combination of the equation 5 with the relation 2 (eq. 2), what is possible on the assumption that $\mu_i = \bar{\mu}_{ss}$ for the given RH, leads to the following expression:

$$\bar{\mu}_{ss-RH} = \frac{1}{(N - N_{ss})} * \sum_{i=N_{ss}}^N C_{\bar{\mu}_{ss}}(RH(i)) + \bar{\mu}_{ss-0} \quad (\text{eq. 6}).$$

Figure 13 compares the experimental values of average steady state coefficient of friction ($\bar{\mu}_{\text{exp.ss-RH}}$) defined from the equation 5 to the theoretical prediction (theoretical average steady-state coefficient of friction ($\bar{\mu}_{\text{th.ss-RH}}$)) calculated from the equation 6. The best prediction is achieved when the theoretical values of average steady-state coefficient of friction are identical to the experimental ones. A linear fitting for the points using the sum of the least squares has been performed and compared with the assumed perfect predictions. It turns out that the introduced ‘composite’ formulation (eq. 6) does not permit an accurate prediction, because the obtained goodness-of-fit defined by the coefficient of determination for the approximated linear regression (made for the correlated data) is very low ($R^2=0.23$). Experimental and theoretical values of average steady-state coefficient of friction for the fretting tests under variable relative humidity conditions are compiled in Table V.

3. 2. 3 Wear behaviour

It has been shown that the prediction of wear kinetic based on a single energy wear coefficient is stable only for a narrow interval of the relative humidity. With exception of some stabilized domain observed for RH values greater than 70%, a specific energy wear coefficient corresponding to each relative humidity interval has to be considered. Therefore, it is necessary to put forward the question: how to quantify the fretting wear kinetics under variable relative humidity? In order to solve such a complex problem, a ‘composite’ wear law integrating the wear energy coefficient as a function of the applied relative humidity ($\alpha(\text{RH}_i)$) is considered. Taking into account an additive property of the dissipated energy it is assumed that the total wear achieved under variable relative humidity (theoretical wear volume: $V_{\text{th.}}$) is the sum of the elementary contributions for each relative humidity. The following linear formulation can then be introduced:

$$V_{th.} = \sum_{i=1}^N \alpha(RH_i) * E_d(i) \quad (\text{eq. 7}),$$

with $E_d(i)$ – the cumulated dissipated energy corresponding to the adequate $\alpha(RH_i)$ value. Figure 14 depicts the comparison of the experimental wear volumes ($V_{exp.}$) obtained under variable relative humidity (Fig. 3), to the predicted wear volumes ($V_{th.}$) extrapolated from the proposed ‘composite’ wear formulation (eq. 7). An optimal prediction is achieved when the theoretical wear volumes are identical to the experimental ones. As it is illustrated in the Figure 14 a rather good correlation can be observed. A linear fitting for the points using the sum of the least squares has been performed and compared with the assumed perfect predictions. It turns out that the introduced ‘composite’ wear law depicts a rather high convergence (0.98) with the experimental results. Such a linear regression displays also a high stability ($R^2=0.86$) and a rather low dispersion (<25%).

Experimental and theoretical values of wear volume for the fretting tests under variable relative humidity conditions are provided in Table V.

Therefore, it can be concluded that in spite of the simplicity, the proposed linear ‘composite’ energy wear formulation provides a good prediction of the wear behaviour under variable and complex relative humidity conditions. It again supports the additive properties of the considered energy wear concept.

4. Discussion and conclusions

The results show that the relative humidity affects significantly the friction behaviour of the alumina-TiN tribo-system under fretting wear involving complex tribochemical reactions. An increase of the RH promotes the formation of hydrate structures in the contact and modifies the third body rheology. Those act as a solid lubricant contributing to decrease of shear forces in the contact. A linear dependence of the coefficient of friction has been established and formalized. The presence of nitrogen in the wear debris has been observed

earlier by other researchers [4, 11]. It suggests that rather Ti-O-(N) complex amorphous structures [4], than only TiO₂ phases, are generated through the interface. The given TEM diffraction pattern confirms this aspect.

The expected tribological behaviour, for which an increase of the friction force leads to an increase of the wear rate, has not been confirmed in the work. This unexpected result suggests that not only the mechanical damage is involved in the overall fretting degradation process of the coating and a tribochemical aspect must be considered as well. Hence, it can be assumed that even if the shear stress intensity is reduced under moist conditions, an increase of humidity will favour the tribo-oxidation of TiN coating and finally increase the energy wear rate. A second hypothesis, developed by Liskiewicz et al. [5], suggests that an increase of the relative humidity value favours characteristic W-shape wear scar geometry (Fig. 15), due to a specific adhesion of the third body layer on to the alumina counter-body. Such interface morphology tends to concentrate the loadings on the external part of the contact promoting higher shear stress discontinuity. Such highest local stress loadings are then assumed to increase the wear kinetics.

Wear results under constant relative humidity conditions depicts a significant dependence of the energy wear coefficient with the applied relative humidity. A parabolic increase of the energy wear rate with the relative humidity has been found and formalized. Such a result seems to contradict the previous outcomes obtained by Celis et al. [6]. In their work, the authors have suggested a single and unique energy wear coefficient to describe the overall wear behaviour independently of the relevant relative humidity. However, it should be noticed that those results have been obtained for the significantly lower normal load of 1 N and a very small contact area. It has been shown that relative humidity mainly impacts on the third body nature and rheology. The larger is the contact area, the higher amount of the third body will be trapped through the interface consequently of the relative humidity dependence. It could therefore be explained such apparent disagreement by considering a contact size effect. Such

an interesting conclusion suggests introducing and developing size effect investigations to better formalize tribology phenomena.

The results presented in this work show that the humidity interacts both on the friction and the wear mechanism. The friction analysis under variable relative humidity conditions outlines complex third body transitions, which requires specific attentions to be fully understood and quantified. As it turned out the introduced 'composite' formulation does not allow an accurate prediction of the average steady-state coefficient of friction under variable relative humidity conditions. Basically, most points in Fig. 13 lie above straight dashed line, displaying optimal prediction, what is close related to the 'friction memory effect' as well as the complex third body transfer occurring after each RH transition.

Regarding wear, it turns out that the energy approach based on a single energy wear coefficient is stable only for constant RH conditions. It cannot be extrapolated for variable RH conditions, as it does not take into account the variation of the tribochemical response of the system. In order to evaluate the wear response of the TiN coating under variable relative humidity, a simple 'composite' wear law, integrating the energy wear coefficient as a function of the relative humidity, has been introduced. Based on a plain linear description, it permits a prediction, with a rather good precision, the wear of the TiN coating under variable relative humidity varying from 10 to 90%. It seems that basic formalism may be a promising tool to assess the wear responses under variable environmental conditions. To extend the given description it is necessary to undertake investigations for the other tribo-systems including, for example, an adhesive steel-steel tribo-couple.

Acknowledgments

Authors would like to thank to the Region Rhône-Alpes (France) for the financial support of this work in the frame of the MIRA programme.

References

1. **I. L. Singer, S. Fayeulle and P. D. Ehni**, *Wear* **149** (1991) 375-394
2. **H. Mohrbacher, B. Blanpain, J.-P. Celis and J. R. Roos**, *Wear* **180** (1995) 43-52
3. **E. De Wit, L. Froyen and J.-P. Celis**, *Wear* **221** (1998) 124-133
4. **E. De Wit, B. Blanpain, L. Froyen and J.-P. Celis**, *Wear* **217** (1998) 215-224
5. **T. Liskiewicz, R. Rybiak, S. Fouvry and B. Wendler**, *Journal of Engineering Tribology*, **220 J** (2006), (in press)
6. **M. Z. Huq and J.-P. Celis**, *Wear* **252** (2002) 375-383
7. **S.-Y. Yoon, M.-Ch. Kang, S.-Ch. Kwon and K. H. Kim**, *Surface and Coatings Technology* **157** (2002) 144-150
8. **S. Wilson and A. T. Alpas**, *Wear* **245** (2000) 223-229
9. **D. Klaffke and A. Skopp**, *Surface and Coatings Technology* **98** (1998) 953-961
10. **S. Fouvry, Ph. Kapsa, H. Zahouani and L. Vincent**, *Wear* **203-204** (1997) 393-403
11. **R. G. Vitchev, B. Blanpain and J.-P. Celis**, *Wear* **231** (1999) 220-227
12. **T. Aizawa, A. Mitsuo, S. Yamamoto, T. Sumitomo and S. Muraishi**, *Wear* **259** (2005) 708-718
13. **M. Z. Huq and J.-P. Celis**, *Wear* **225-229** (1999) 53-64
14. **H. Mohrbacher, B. Blanpain, J.-P. Celis, J. R. Roos, L. Stals and M. Van Stappen**, *Wear* **188** (1995) 130-137
15. **H. Chen, P. Q. Wu, C. Quaeyhaegens, K. W. Xu, L. M. Stals, J. W. He and J.-P. Celis**, *Wear* **253** (2002) 527-532
16. **J. Wei., S. Fouvry, Ph. Kapsa and L. Vincent**, *Surface Engineering* **13** (1997) 227-232
17. **S. Wilson and A. T. Alpas**, *Surface and Coatings Technology* **94-95** (1997) 53-59
18. **A. Ramalho and J.-P. Celis**, *Surface and Coatings Technology* **155** (2002) 169-175
19. **J. F. Archard**, *J. Appl. Phys.* **24** (1953) 981-988
20. **X. Qiu and M. E. Plesha**, *Trans. ASME J. Tribol.* **111** (1991) 442-451
21. **S. Fouvry, Ph. Kapsa and L. Vincent**, *Wear* **200** (1996) 186-205

Table I Mechanical and surface properties of the materials used in the study

Materials	Thickness T [μm]	Hardness H	Young's modulus E [GPa]	Poisson ratio ν	Surface roughness R_a [μm]
<i>Vanadis 23</i>	-	64 HRC	230	0.3	0.2
<i>Alumina</i>	-	2300 HV _{0.1}	370	0.27	0.01
<i>TiN</i>	4.0	2000 HV _{0.05}	600	0.25	0.2

Table II Detailed data concerning conditions of the test carried out under variable RH

Tests type A						
	N_i , with: N - number of cycles for given relative humidity, i - relative humidity value [%].					Total No. of cycles
<i>Test No.</i>	N_{10}	N_{30}	N_{50}	N_{70}	N_{90}	ΣN_i
1	4000	2000	2000	2000	3000	13000
2	3000	1000	1000	1000	1500	7500
3	7000	-	-	-	3000	10000
4	-	4500	-	1500	-	6000
5	-	6000	1500	2500	-	10000
Tests type B						
<i>Test No.</i>	N_{90}	N_{70}	N_{50}	N_{30}	N_{10}	ΣN_i
1	4000	2000	2000	2000	3000	13000
2	3000	1000	1000	1000	1500	7500
3	7000	-	-	-	3000	10000
4	-	4500	-	1500	-	6000
5	-	6000	1500	2500	-	10000
Tests type C						
<i>Test No.</i>	N_{90}	N_{10}	N_{90}	N_{10}		ΣN_i
1	5000	2500	2500	2500	-	12500
	N_{70}	N_{30}	N_{70}	N_{30}		ΣN_i
2	4500	2000	2000	2000	-	10500
Tests type D						
<i>Test No.</i>	N_{10}	N_{90}	N_{10}	N_{90}		ΣN_i
1	5000	2500	2500	2500	-	12500
	N_{30}	N_{70}	N_{30}	N_{70}		ΣN_i
2	4500	2000	2000	2000	-	10500

Table III Average steady-state coefficients of friction for the constant relative humidity conditions

Relative humidity RH [%]	<i>10</i>	<i>30</i>	<i>50</i>	<i>70</i>	<i>90</i>
Average steady-state coefficient of friction $\bar{\mu}_{ss}$	0.610	0.563	0.529	0.492	0.469

Table IV Energy wear rates extracted from fretting wear analysis

$\alpha (\mu\text{m}^3\text{J}^{-1})// R^2$				
<i>RH=10%</i>	<i>RH=30%</i>	<i>RH=50%</i>	<i>RH=70%</i>	<i>RH=90%</i>
1575//0.93	3704//0.93	4225//0.95	5186//0.93	5257//0.90

Table V Experimental and predicted (eq. 6 and 7) values of considered tribo-magnitudes for variable relative humidity conditions

Test No.	Experimental average steady-state COF $\bar{\mu}_{exp.ss-RH}$	Theoretical average steady-state COF $\bar{\mu}_{th.ss-RH}$	Experimental wear volume $V_{exp-RH} [10^5 \mu m^3]$	Theoretical wear volume $V_{th-RH} [10^5 \mu m^3]$
A1	0.490	0.523	9.606	8.461
A2	0.569	0.519	4.843	5.038
A3	0.563	0.554	5.277	5.406
A4	0.504	0.532	3.759	4.650
A5	0.553	0.533	9.636	8.557
B1	0.578	0.543	10.618	10.128
B2	0.56	0.547	4.651	5.183
B3	0.556	0.525	6.818	7.797
B4	0.539	0.522	4.417	5.593
B5	0.515	0.523	7.668	8.252
C1	0.595	0.54	9.539	9.218
C2	0.551	0.528	8.045	9.698
D1	0.596	0.54	8.277	7.779
D2	0.544	0.528	8.246	8.977

List of figure captions

- Fig. 1** X-ray diffraction pattern of the TiN coating deposited on the quenched and tempered Vanadis 23 HSS steel substrate
- Fig. 2** Fretting test scheme
- Fig. 3** Patterns of the tests under variable relative humidity conditions
- Fig. 4** Evolution of the coefficient of friction versus the test duration for the tests conducted at 10 and 90% relative humidity
- Fig. 5** The average steady-state coefficient of friction of the alumina-TiN system as a function of the relative humidity
- Fig. 6** Wear volume of the studied TiN coating as a function of the accumulated dissipated energy for different relative humidity
- Fig. 7** Evolution of the associated energy wear coefficient defined from Fig. 6 versus RH for the alumina-TiN tribo-couple
- Fig. 8** SEM observations of the third body structures at the borders of the contact just after tests at 10000 cycles for (a) 10% and (b) 90% relative humidity
- Fig. 9** EDX spectrum of the wear debris generated at 10% RH (a) and 90% RH (b)
- Fig. 10** TEM bright field image of the particle generated during the test at 10% RH (a) and 90% RH (d); ESI of the particle separated from the wear debris – distribution of Ti and O for 10% RH (b), (c) and 90% RH (e), (f) respectively
- Fig. 11** TEM diffraction patterns of the wear debris obtained under fretting wear test at 10% RH and at 10000 cycles: (a) just after switching the electron beam on, (b) after 5 minutes irradiation with the electron gun
- Fig. 12** Evolution of the coefficient of friction versus the test duration for variable relative humidity test A1 (a), B1 (b), C1 (c) and D1 (d)

Fig. 13 Comparison between experimental and theoretical (eq. 6) average steady-state coefficients of friction for tests conducted under variable relative humidity conditions

Fig. 14 Wear extension under variable relative humidity conditions: comparison between experimental and predicted (eq. 7) wear volumes

Fig. 15 Surface morphology of coated specimen and alumina counter-body after fretting test:
(a) TiN coating and (b) alumina ball with TiN debris [5]

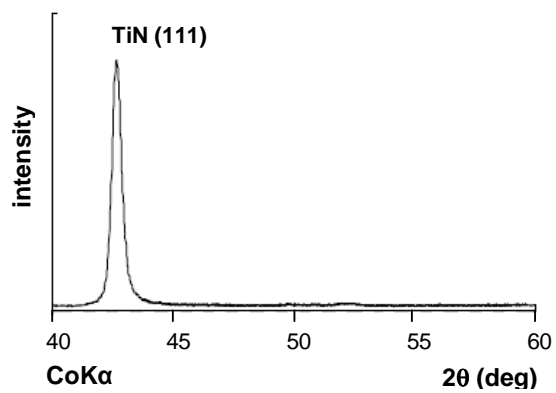


Figure 1

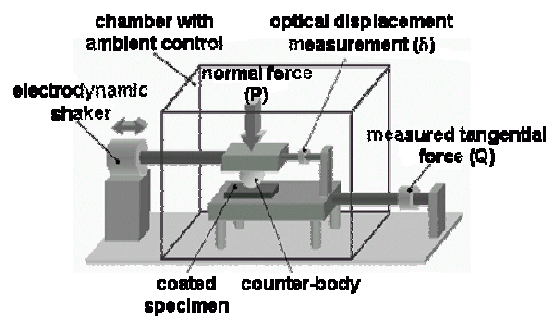


Figure 2

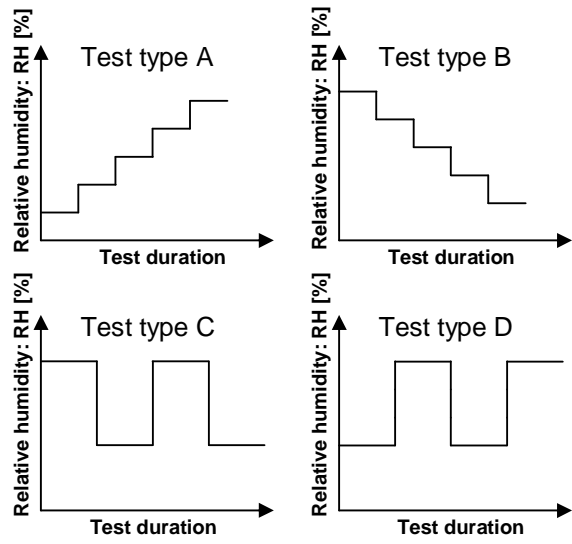


Figure 3

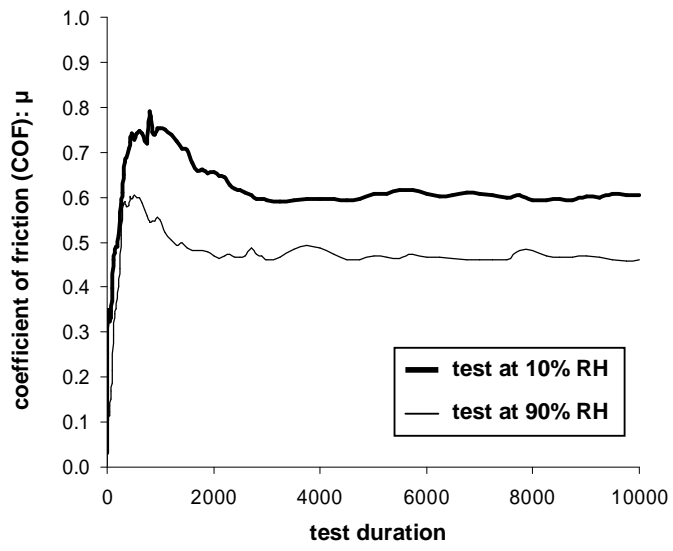


Figure 4

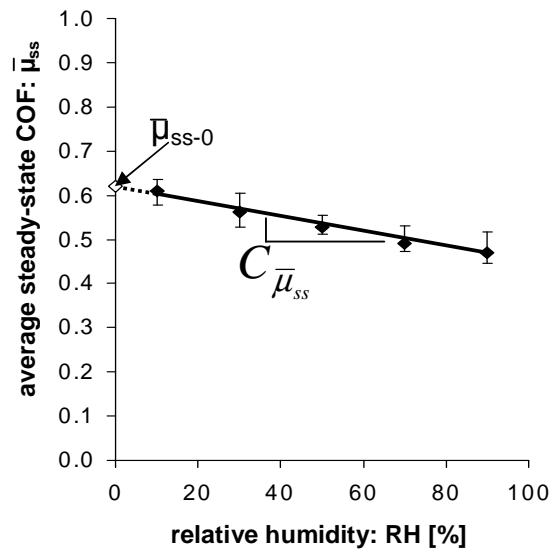


Figure 5

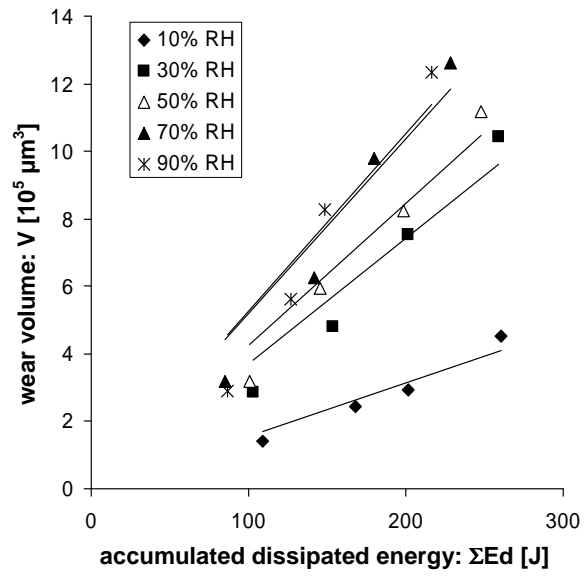


Figure 6

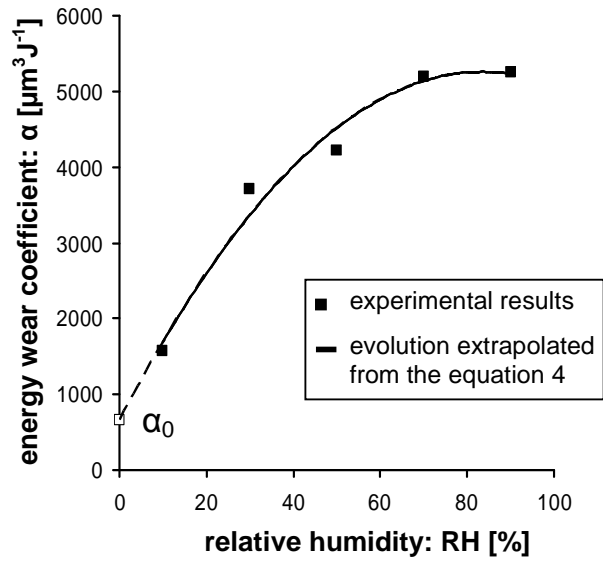


Figure 7

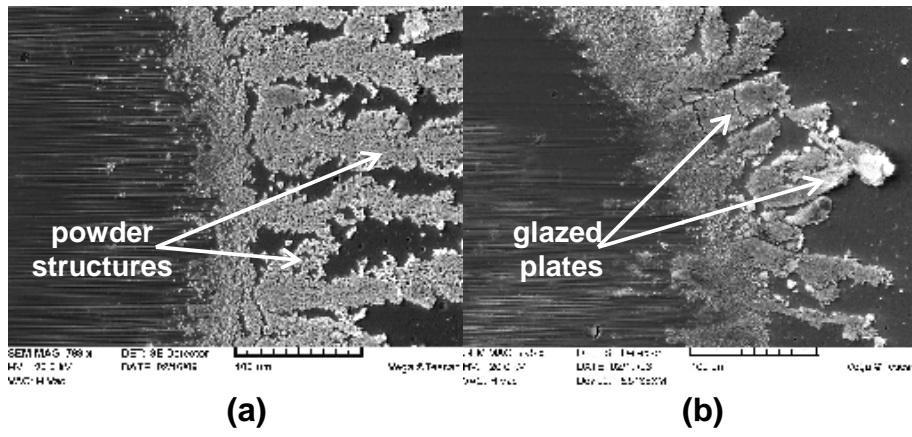


Figure 8

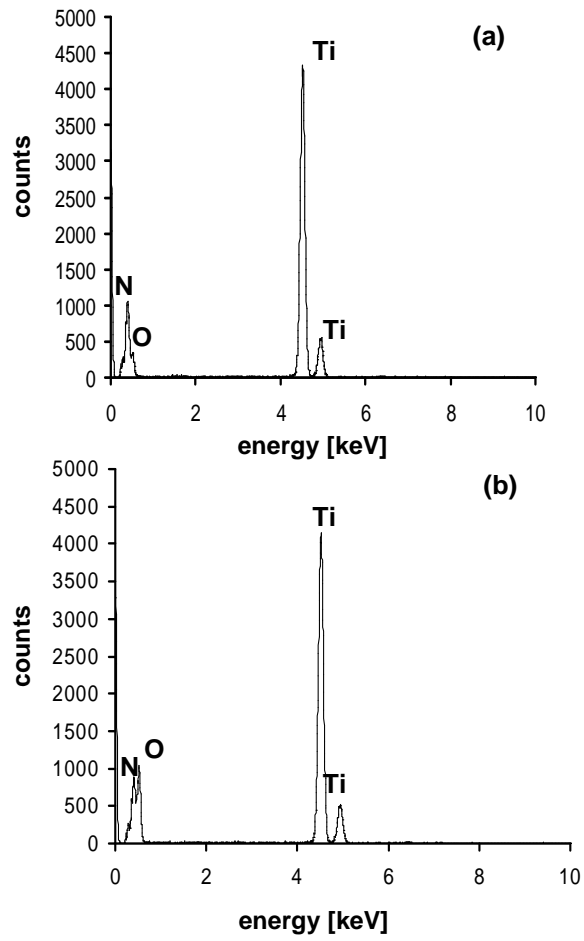


Figure 9

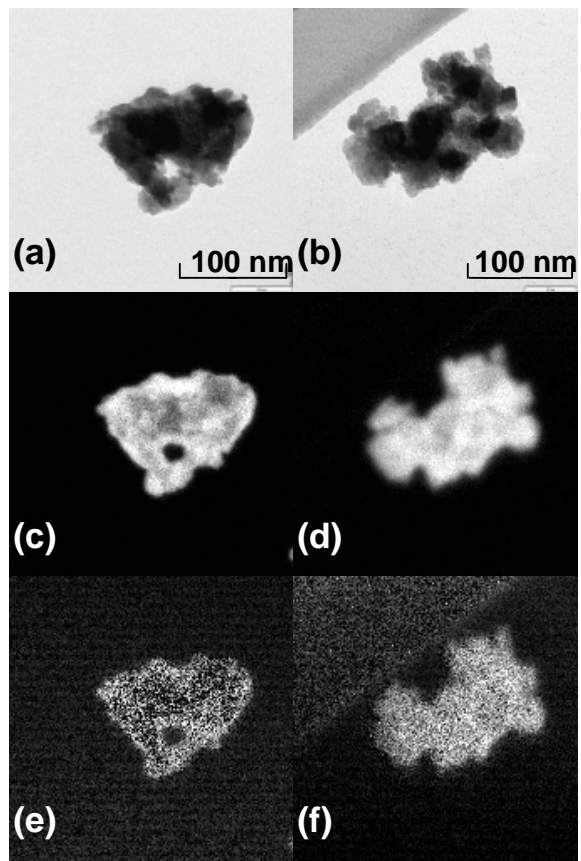
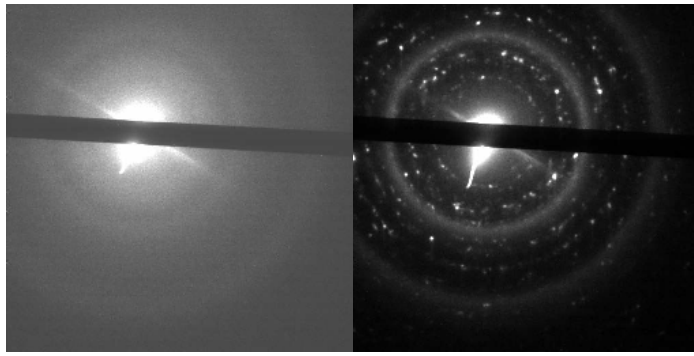


Figure 10



(a)

(b)

Figure 11

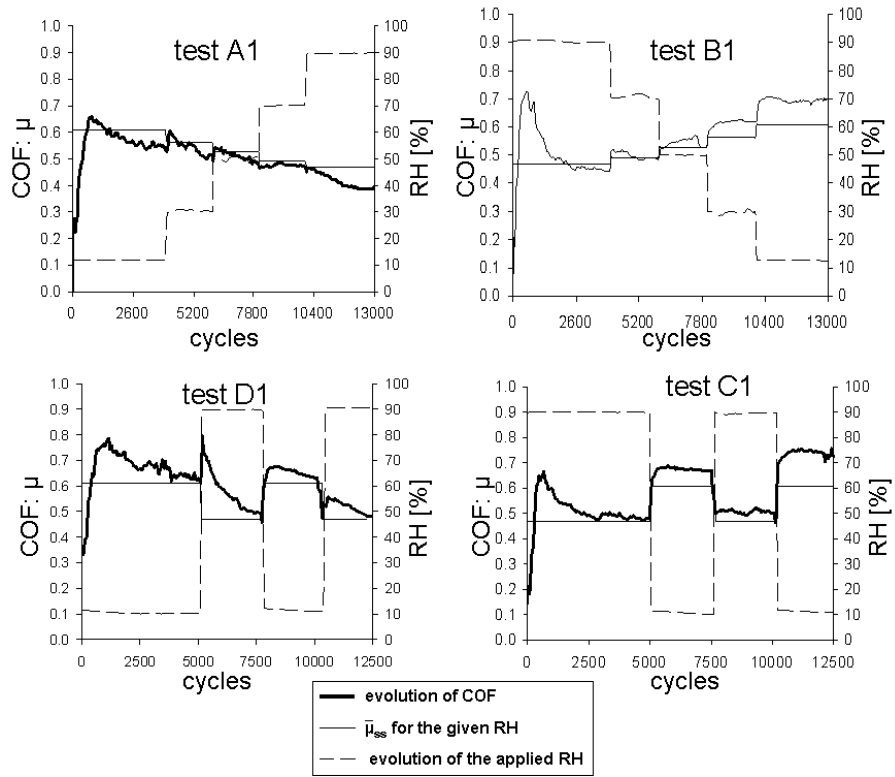


Figure 12

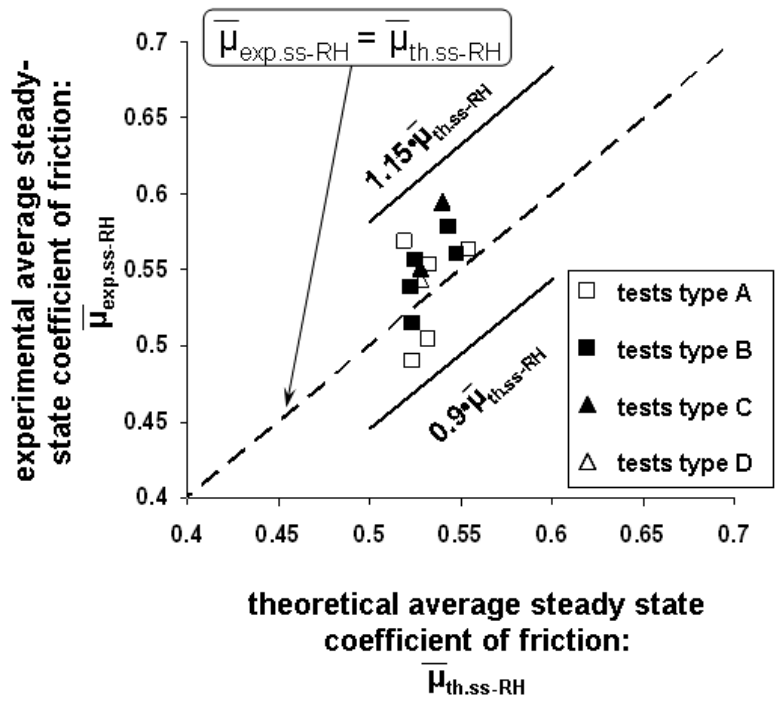


Figure 13

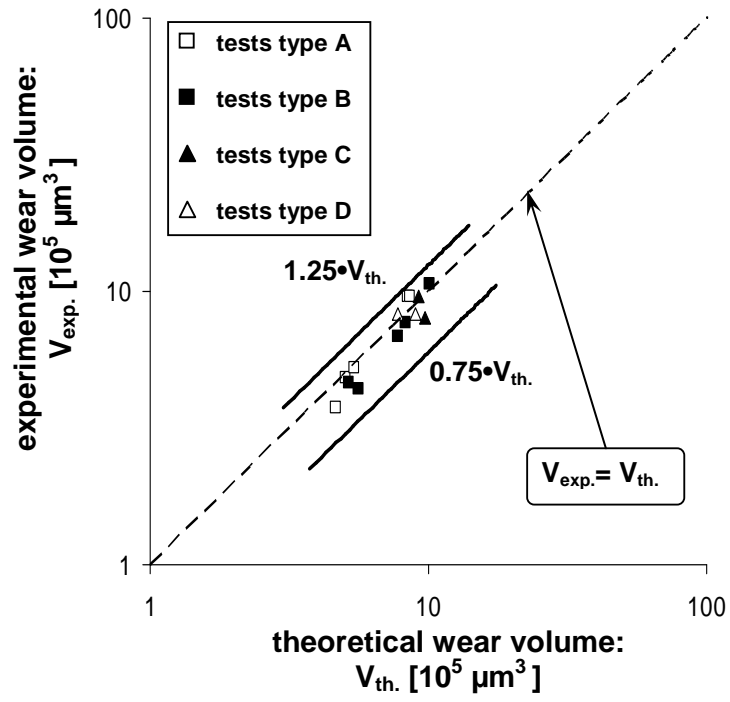


Figure 14

